



Supporting Information

for *Adv. Sci.*, DOI: 10.1002/advs.202001853

Polymeric Nanoparticles with ROS-Responsive Prodrug and Platinum Nanozyme for Enhanced Chemophotodynamic Therapy of Colon Cancer

*Ying Hao, Yuwen Chen, Xinlong He, Yongyang Yu, Ruxia Han, Yang Li, Chengli Yang, Danrong Hu, and Zhiyong Qian**

Polymeric Nanoparticles with ROS-Responsive Prodrug and Platinum Nanozyme for Enhanced Chemo-Photodynamic Therapy of Colon Cancer

Ying Hao,[†] Yuwen Chen,[†] Xinlong He,[†] Yongyang Yu,[‡] Ruxia Han,[†] Yang Li,[†] Chengli Yang,[†] Danrong Hu,[†] Zhiyong Qian^{*,†}

[†]State Key Laboratory of Biotherapy and Cancer Center, West China Hospital, Sichuan University, and Collaborative Innovation Center of Biotherapy, Chengdu, 610041, PR China

[‡]Department of Gastrointestinal Surgery, West China Hospital, Sichuan University, Chengdu, 610041, PR China

* To whom should be corresponded, Tel/Fax: +86-28-85557632, E-mail: anderson-qian@163.com (Qian ZY).

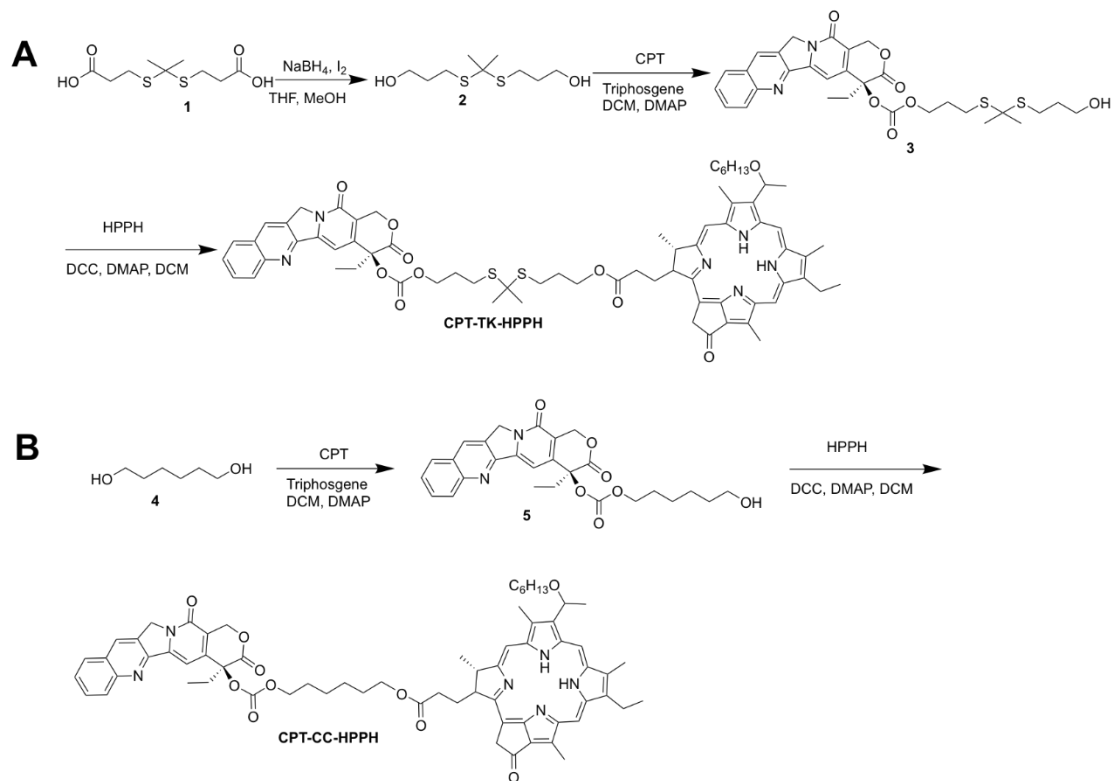


Figure S1. Synthesis method for (A) CPT-TK-HPPH and (B) CPT-CC-HPPH.

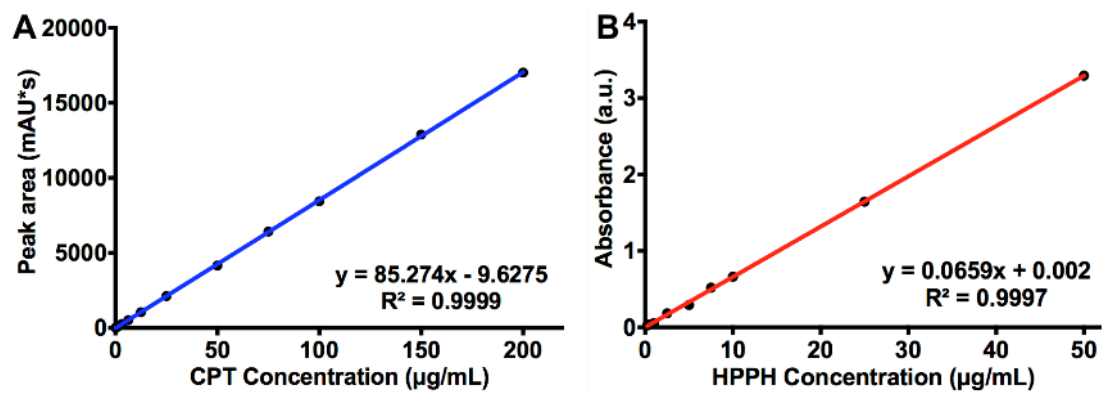


Figure S2. Linear correlation of (A) CPT and (B) HPPH against its corresponding concentrations (inset: the linear fitting equation).

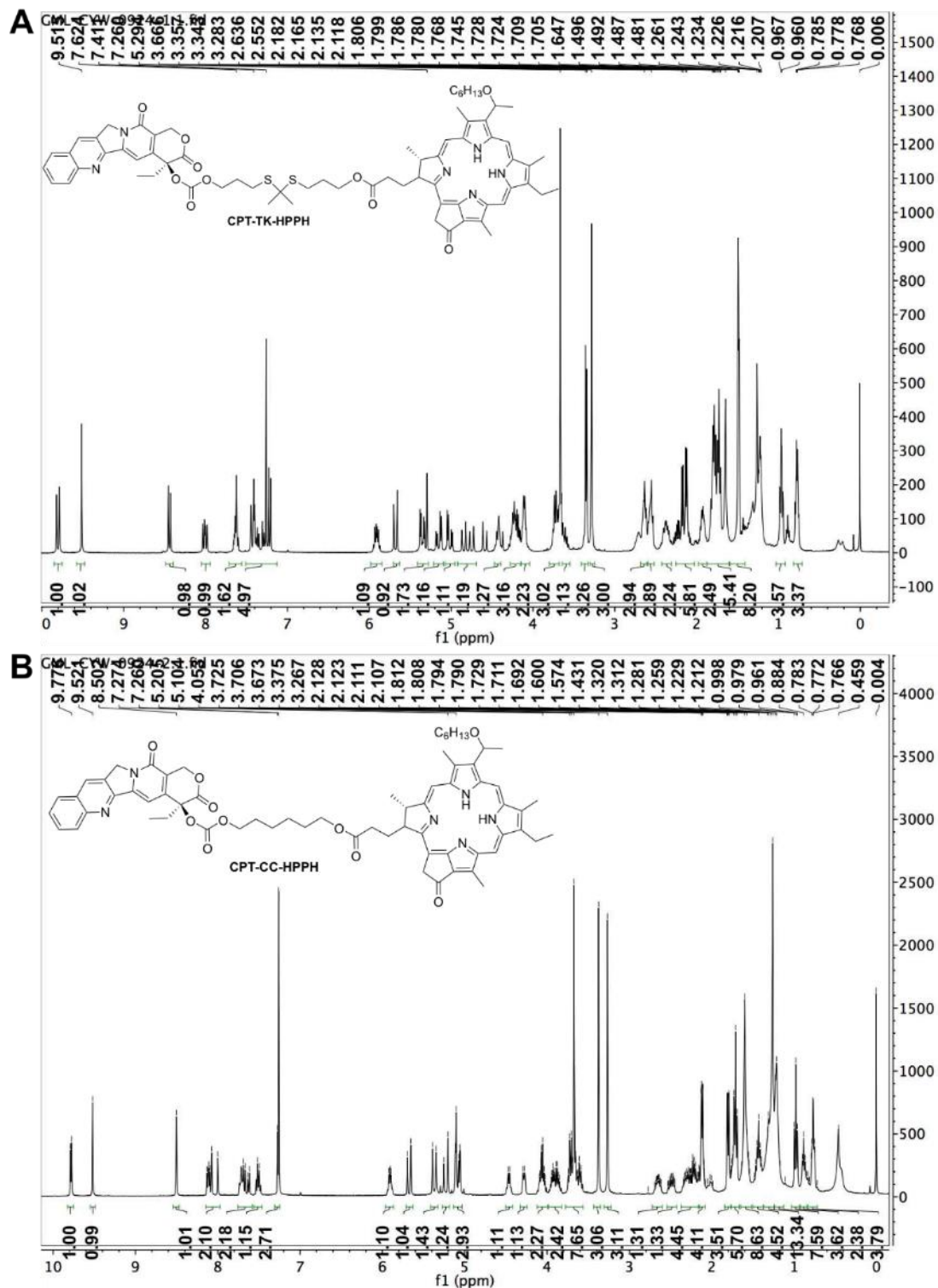


Figure S3. ¹H NMR spectra of (A) CPT-TK-HPPH and (B) CPT-CC-HPPH.

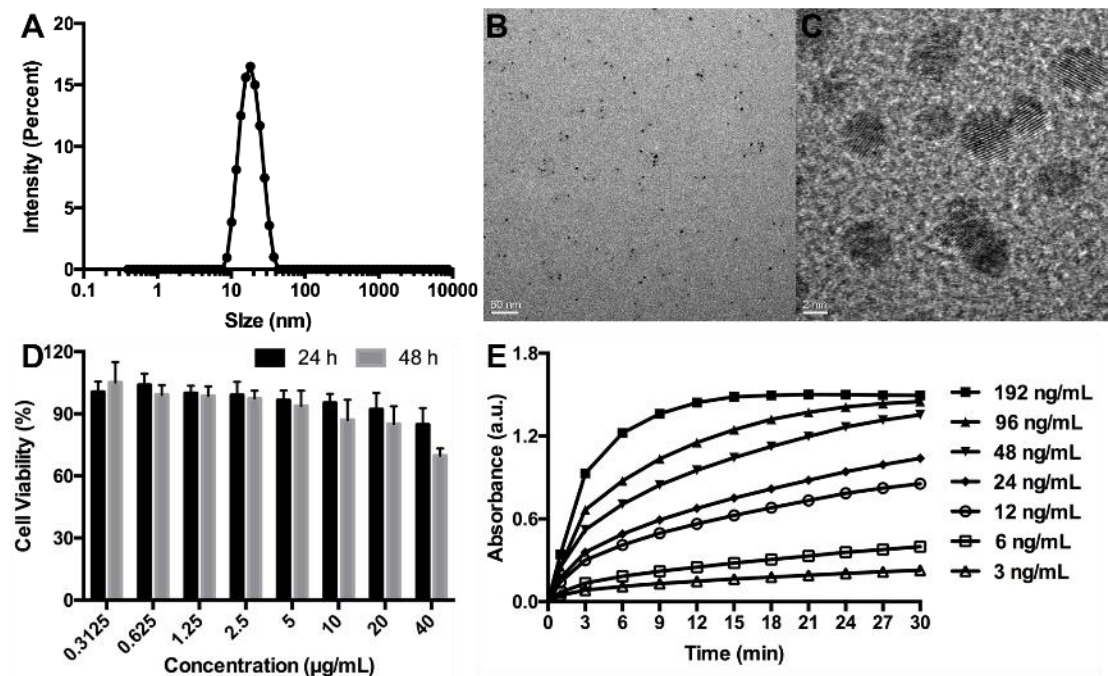


Figure S4. Characterization of PtNP. (A) Particle size, (B, C) TEM image, (D) *in vitro* cell viability of PtNP, and (E) the absorbance evolution for different concentrations of PtNP at 652 nm. Data in (D) and (E) are presented as mean \pm SD ($n = 6$).

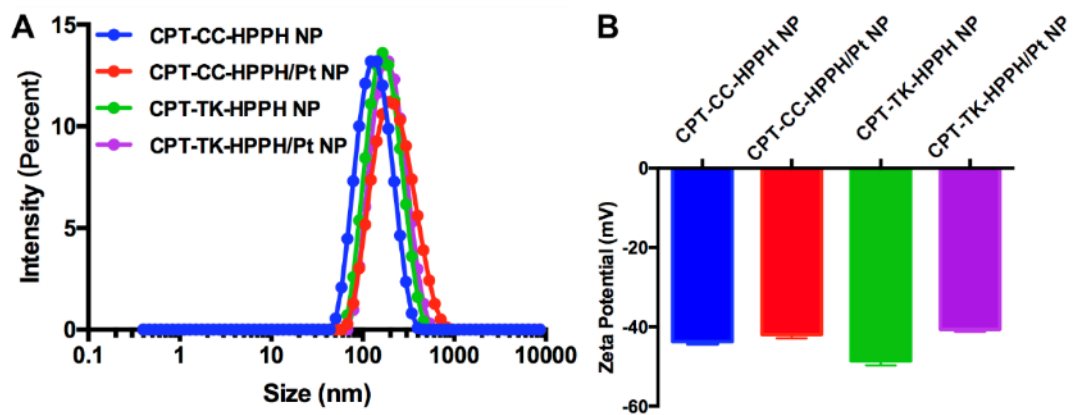


Figure S5. (A) Particle size and (B) zeta potential of CPT-CC-HPPH NP, CPT-CC-HPPH/Pt NP, CPT-TK-HPPH NP, and CPT-TK-HPPH/Pt NP. All quantitative data are presented as mean \pm SD ($n = 3$).

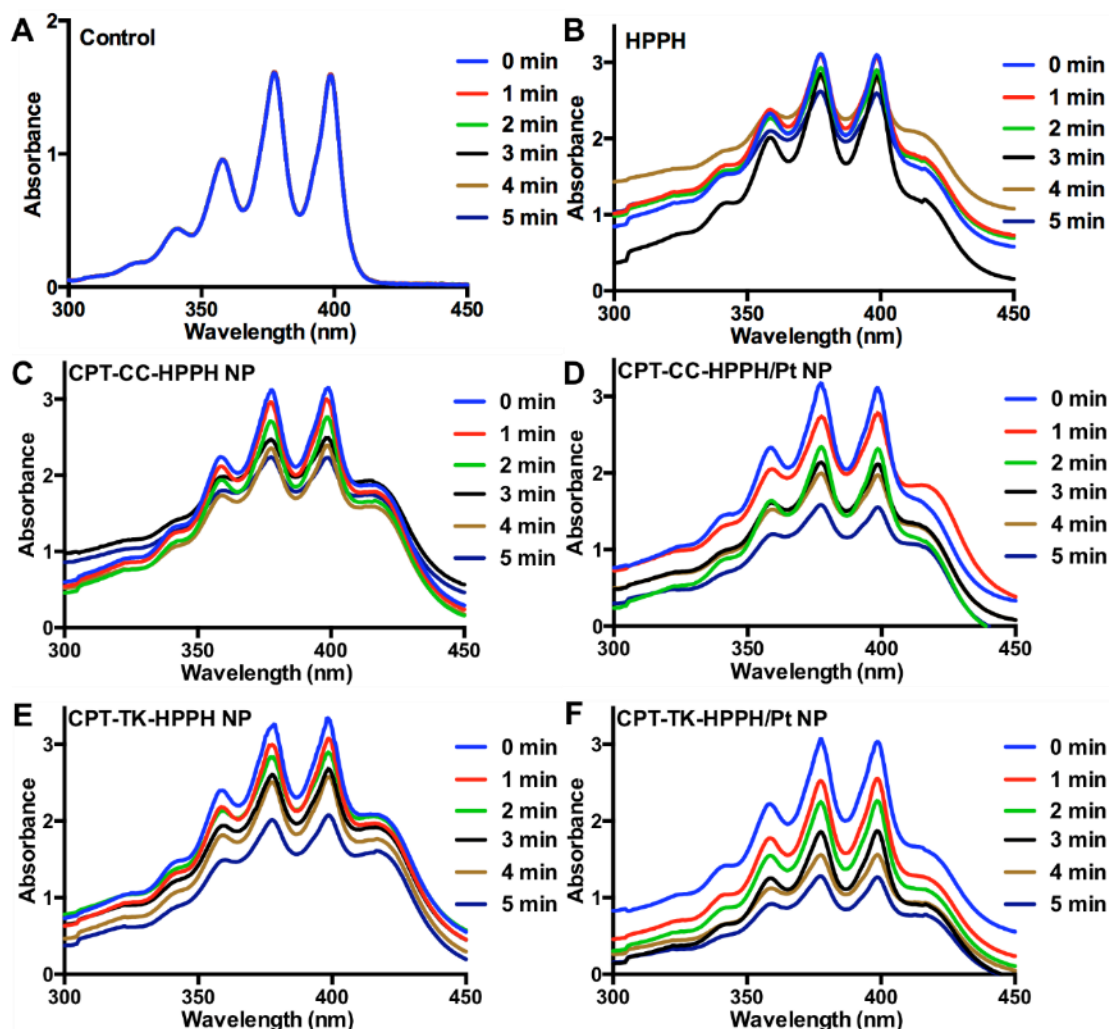


Figure S6. The UV-vis absorption spectra of ABDA in (A) control, (B) HPPH, (C) CPT-CC-HPPH NP, (D) CPT-CC-HPPH/Pt NP, (E) CPT-TK-HPPH NP, and (F) CPT-TK-HPPH/Pt NP group with $100 \mu\text{M}$ H_2O_2 at designated time irradiation for 660 nm laser.

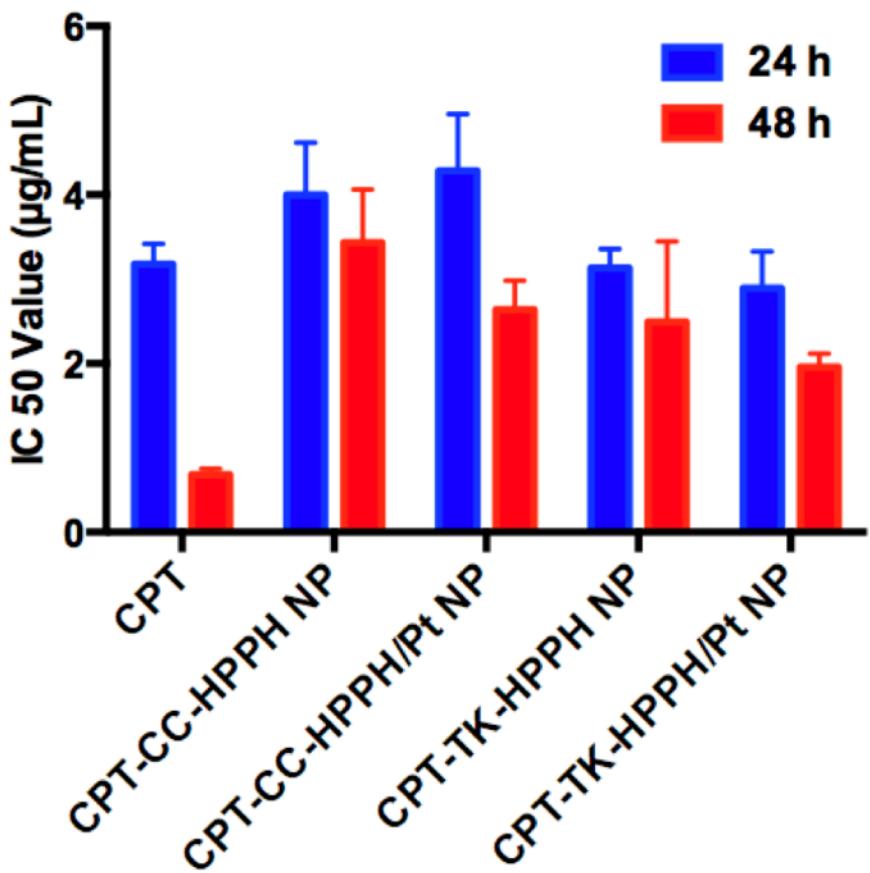


Figure S7. IC₅₀ value of CPT, CPT-CC-HPPH NP, CPT-CC-HPPH/Pt NP, CPT-TK-HPPH NP, and CPT-TK-HPPH/Pt NP. The data are presented as mean \pm SD (n = 6).

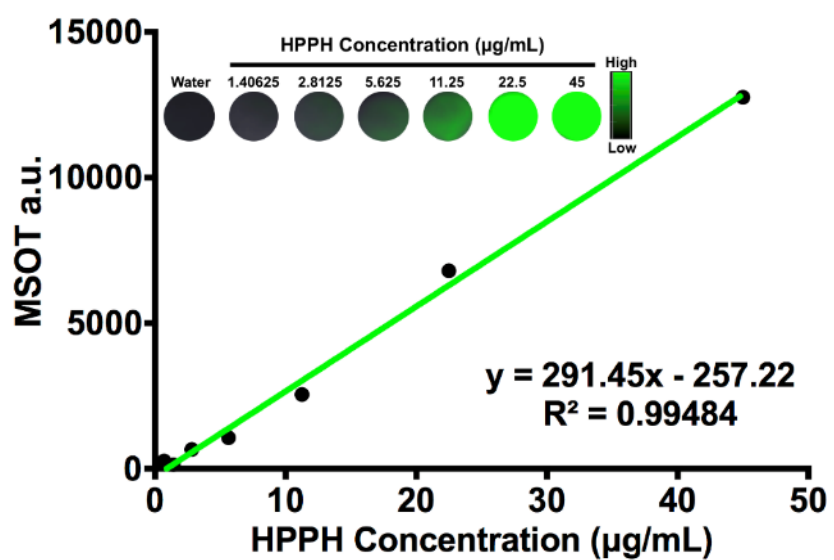


Figure S8. (A) Linear correlation of PA signals of HPPH in CPT-TK-HPPH/Pt NP against its corresponding concentrations. PA imaging of CPT-TK-HPPH/Pt NP at indicated HPPH concentrations at 680 nm, with the linear fitting equation inserted.

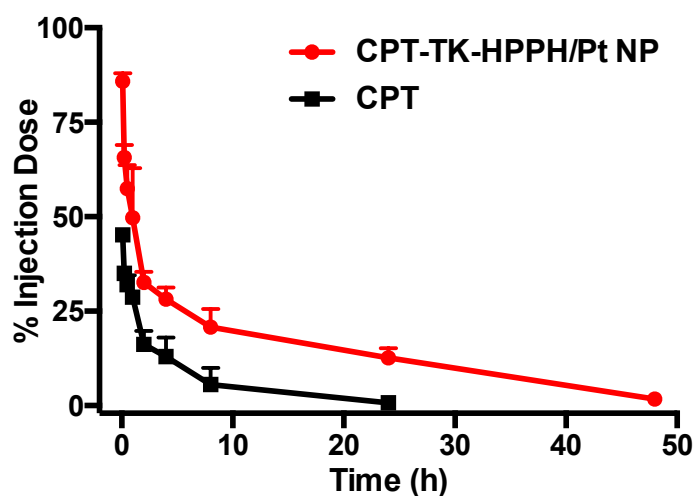


Figure S9. Plasma concentration-time profiles of CPT-TK-HPPH/Pt NP and CPT in rats after intravenous injection. The data are presented as mean \pm SD ($n = 3$).

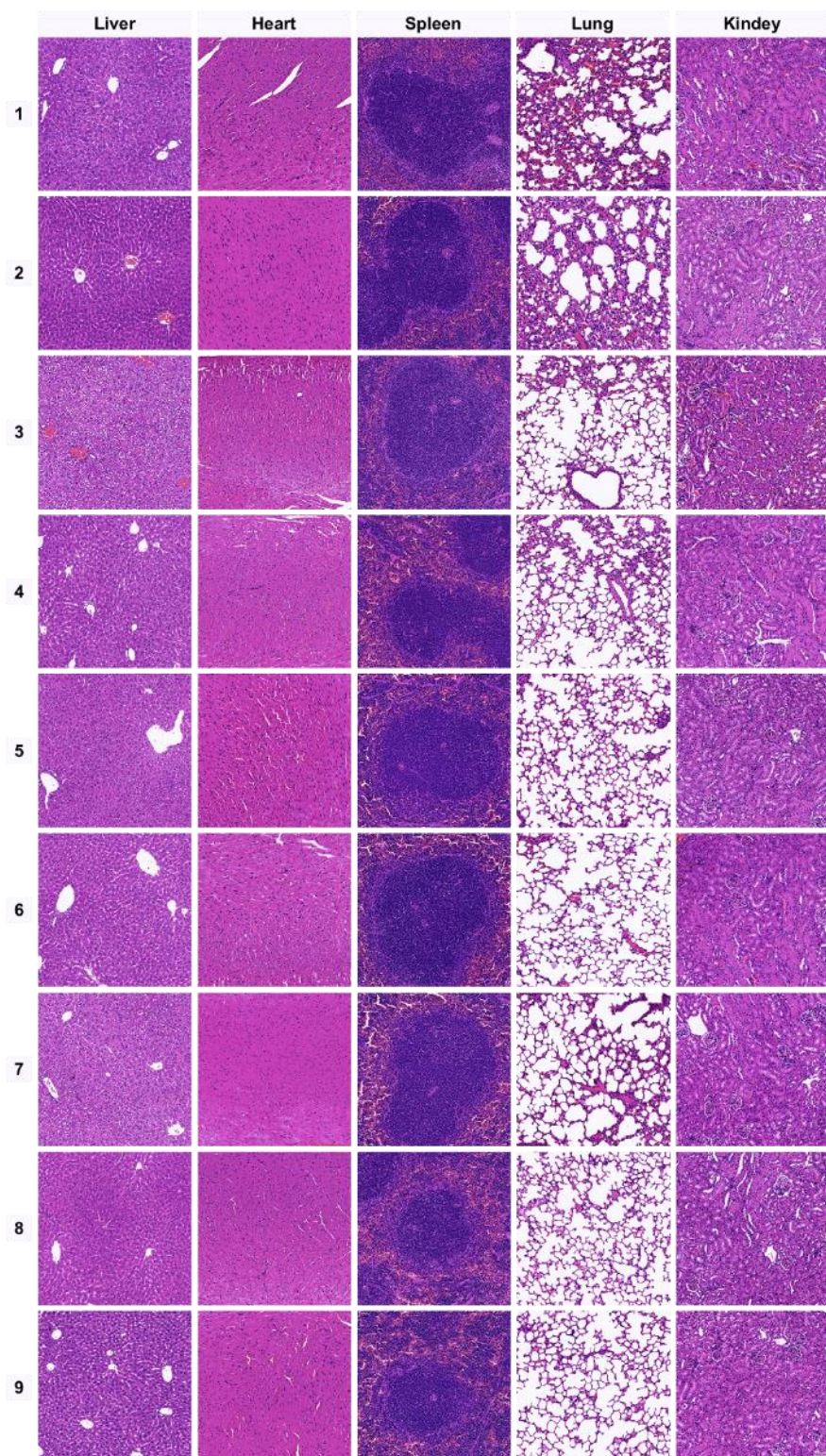


Figure S10. Representative H&E stained images of the liver, heart, spleen, lung, and kidney tissues (scale bar, 50 μ m) of CT26 tumor-bearing mice. (1. Control, 2. Control+Laser, 3. CPT, 4. HPPH+Laser, 5. CPT-CC-HPPH/Pt NP+Laser, 6. CPT-TK-HPPH NP, 7. CPT-TK-HPPH NP+Laser, 8. CPT-TK-HPPH/Pt NP, 9. CPT-TK-HPPH/Pt NP+Laser.)

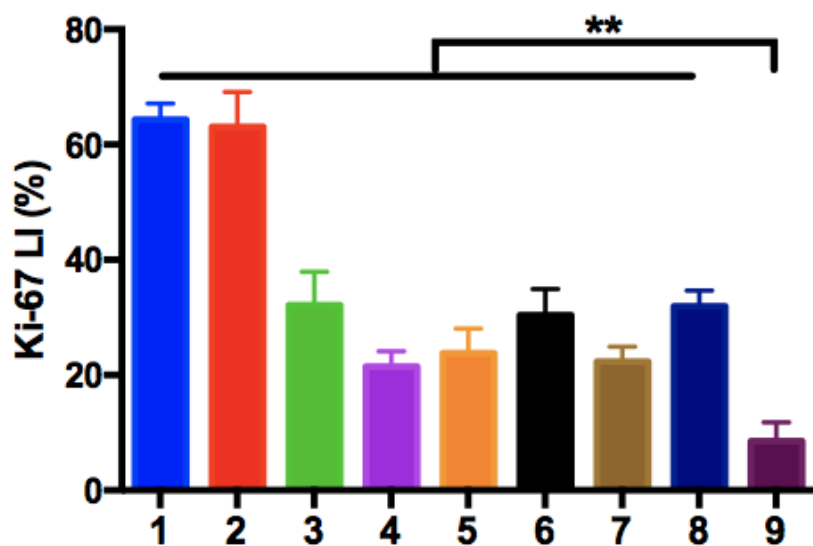


Figure S11. Ki-67 LI of tumors in each group. The data are presented as mean \pm SD ($n = 5$). “**” means the $P < 0.01$. (1. Control, 2. Control+Laser, 3. CPT, 4. HPPH+Laser, 5. CPT-CC-HPPH/Pt NP+Laser, 6. CPT-TK-HPPH NP, 7. CPT-TK-HPPH NP+Laser, 8. CPT-TK-HPPH/Pt NP, 9. CPT-TK-HPPH/Pt NP+Laser.)

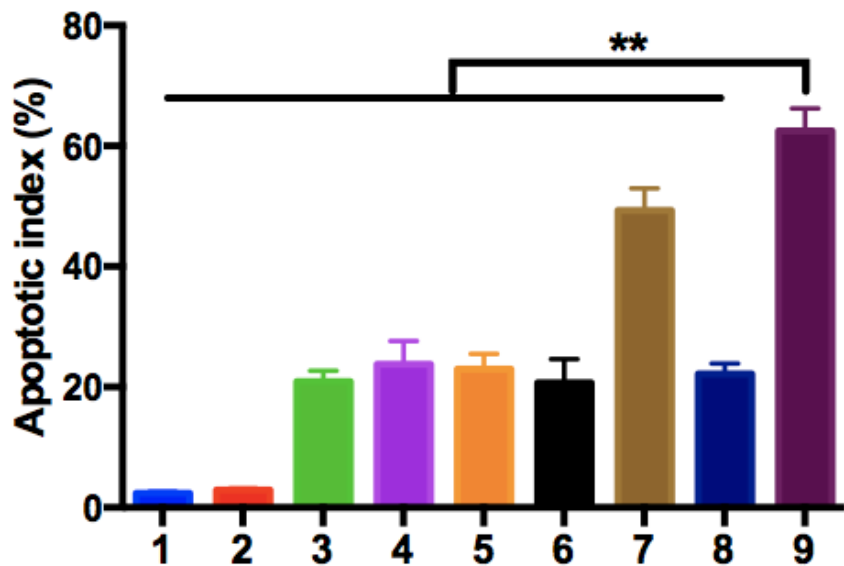


Figure S12. Apoptotic index of tumors in each group. The data are presented as mean \pm SD ($n = 5$). “**” means the $P < 0.01$. (1. Control, 2. Control+Laser, 3. CPT, 4. HPPH+Laser, 5. CPT-CC-HPPH/Pt NP+Laser, 6. CPT-TK-HPPH NP, 7. CPT-TK-HPPH NP+Laser, 8. CPT-TK-HPPH/Pt NP, 9. CPT-TK-HPPH/Pt NP+Laser.)